Materials Letters 115 (2014) 49–52

Contents lists available at ScienceDirect

Materials Letters

journal homepage: www.elsevier.com/locate/matlet

Enhanced electrochemical performance in $LiNi_{0.8}Co_{0.15}Al_{0.05}O_2$ cathode material: Resulting from Mn-surface-modification using a facile oxidizing–coating method

Bin Huang, Xinhai Li*, Zhixing Wang, Huajun Guo, Zhenjiang He, Renheng Wang, Jiexi Wang, Xunhui Xiong

School of Metallurgy and Environment, Central South University, Changsha 410083, China

ARTICLE INFO

Article history:
Received 6 July 2013
Accepted 1 October 2013
Available online 10 October 2013

Keywords:
Energy storage and conversion
Lithium ion batteries
Electrode materials
Surfaces

ABSTRACT

Mn-surface-modified $LiNi_{0.8}Co_{0.15}Al_{0.05}O_2$ cathode material is successfully prepared from a Mn-containing $Ni_{0.8}Co_{0.15}Al_{0.05}(OH)_2$ precursor, which is obtained through a novel oxidizing–coating method based on the reaction between MnO_4^- and Ni^{2+}. The structure and morphology of the as-prepared sample are characterized by XRD and SEM respectively; the distribution of Mn is detected by EDS mapping. Compared with pristine sample, the Mn-surface-modified one shows no change in crystal structure or microstructure. By electrochemical characterizations, it is proved that the capacity retention delivered by the Mn-surface-modified sample is remarkably enhanced compared with that of the pristine one. At 2*C*, the pristine and Mn-surface-modified samples exhibit their respective capacity retentions of 50.9% and 62.9% after 200 cycles at room temperature and the ones of 49.3% and 67.5% after 100 cycles at 55 °C. Furthermore, from the EIS results, the Mn-surface-modified sample is proved to have lower aging rate.

1. Introduction

Because of the unstable Ni^{4+} ions, the issue of fast aging rate and thermal instability of the $LiNiO_2$-based materials still deserves concern, and this problem will be more serious when the Ni content is fairly high ($x \leq 0.2$ in $Li[Ni_{1-x}M_x]O_2$) [1]. Among the Ni-rich materials, $LiNi_{0.8}Co_{0.15}Al_{0.05}O_2$ is one of the most intriguing cathode materials, which exhibits improved electrochemical and thermal properties due to the substitution of Co and Al for Ni sites. However, the capacity fading and resistance increasing of $LiNi_{0.8}Co_{0.15}Al_{0.05}O_2$, which hinder its large scale application, still need to be further suppressed [2].

Many strategies were proposed for enhancing the electrochemical and thermal properties, such as coating [3–6], doping [7,8], synthesis of gradient materials [9,10] and mixing with spinel material [11]. One effective way to suppress the structural changes and collapse is to introduce pillar ions such as Mg^{2+} [12]. Recently, Cho et al. [13] reported a new type of protective surface pillaring layer which was formed via Mn element doping at the surface of $LiNi_{0.70}Co_{0.15}Mn_{0.15}O_2$. In their method, the $Ni_{0.70}Co_{0.15}Mn_{0.15}(OH)_2$ precursor was coated by MnO_2 via a sol–gel process, and the Mn-surface-doped cathode was obtained by annealing the MnO_2-coated precursor and $LiOH \cdot H_2O$. The surface Mn^{4+} was proved to induce the reduction of Ni^{3+} to Ni^{2+}. A part of the Ni^{2+} simultaneously migrates to Li slabs and forms a nanoscaled NiO pillaring layer, which could block the side-reactions between the cathode and electrolyte associated with the structural distortion and capacity fading. In this study, we report a facile process for doping Mn^{4+} at the surface of $LiNi_{0.8}Co_{0.5}Al_{0.05}O_2$ based on the redox reaction between MnO_4^- and Ni^{2+}. In this method, $KMnO_4$ solution is used for treating $Ni_{0.8}Co_{0.15}Al_{0.05}(OH)_2$ which acts as the precursor of $LiNi_{0.8}Co_{0.15}Al_{0.05}O_2$ cathode material. $KMnO_4$ used as not only a Mn source but also an oxidant. The detailed synthesis process is given in the following paper. Meanwhile, the physical and electrochemical characterizations are discussed.

2. Experimental

The pristine $Ni_{0.8}Co_{0.15}Al_{0.05}(OH)_2$ precursor was commercially supplied. The oxidizing–coating process was implemented as below. $KMnO_4$ powder was dissolved in deionized water to form a 0.1 mol L^{-1} solution. Subsequently, 5 g $Ni_{0.8}Co_{0.15}Al_{0.05}(OH)_2$ precursor was dispersed in deionized water, followed by dripping 10 mL of the as-prepared $KMnO_4$ solution with magnetic stirring. On the surface of the precursor, Ni^{2+} was immediately oxidized to Ni^{3+}, accompanied by the precipitation of Mn-containing oxides. As a result, the dark green solid powder changed to dark brown.

* Corresponding author. Tel./fax: +86 731 88836633.
E-mail addresses: xinhaili_csu@126.com (X. Li), wangjiexikeen@csu.edu.cn (Z. Wang).

0167-577X/$ - see front matter © 2013 Elsevier B.V. All rights reserved.
http://dx.doi.org/10.1016/j.matlet.2013.10.014

After reaction, the dark brown powder was recovered by filtration, washed three times with deionized water and dried at 110 °C overnight. Finally, the Mn-containing $Ni_{0.8}Co_{0.15}Al_{0.05}(OH)_2$ (the surface compound maybe $Ni_{0.8}Co_{0.15}Al_{0.05}OOH$) and $LiOH{\cdot}H_2O$ were thoroughly mixed with a molar ratio of 1:1.05 before being sintered at 750 °C for 15 h under flowing oxygen. For comparison, a pristine sample was obtained by annealing untreated $Ni_{0.8}Co_{0.15}Al_{0.05}(OH)_2$ and $LiOH{\cdot}H_2O$ with the same molar ratio and sintering process. The sample synthesized by $KMnO_4$ treated precursor was labeled as T-NCA and the pristine one was labeled as U-NCA.

X-ray diffraction (XRD) patterns were measured using a Rigaku Rint-2000 diffractometer with Cu-Kα radiation (1.54056 Å). The morphologies of the as-prepared samples were observed by a scanning electron microscope (FEI, Quanta FEG 250).

CR 2025 coin-type cells were assembled with metallic lithium anodes for electrochemistry studies. The positive electrode was composed of 80 wt% as-prepared sample, 10 wt% Super P carbon black and 10 wt% poly(vinylidene fluoride). The cells were assembled in an Ar-filled glove box (Mikrouna) and cycled between 2.8 and 4.3 V in the galvanostatic mode at a desired *C*-rate (1*C* corresponds to 200 mA g^{-1}). Electrochemical impedance spectroscopy (EIS) was also carried out after different cycle numbers. Before the EIS measurement, all of the cells were charged to 4.0 V to obtain an identical status. The sinusoidal excitation voltage applied to the cells was 5 mV with a frequency range of between 0.01 Hz and 100 kHz.

3. Results and discussion

The XRD patterns of pristine and $KMnO_4$ treated $Ni_{0.8}Co_{0.15}Al_{0.05}(OH)_2$ are presented in Fig. 1a. It can be seen that the diffraction peak positions of the $KMnO_4$ treated precursor fit well with the ones of pristine precursor, which are indexed to $Ni(OH)_2$. Fig. 1b shows the XRD patterns of U-NCA and T-NCA. Both samples are single phase and isostructural with $LiNiO_2$, which adopts $R\bar{3}m$ space group. The results indicate that no structural change has taken place in both the precursor and final product.

Fig. 2 shows the energy dispersive spectrometer (EDS) spectra of the $KMnO_4$ treated precursor and the corresponding T-NCA sample, together with the SEM images and EDS mappings of Mn. It can be seen that Mn has been detected on the surface of the precursor and T-NCA sample. The insets of Fig. 2a and b present the SEM images and EDS mappings of Mn, respectively. The $KMnO_4$ treated precursor shows a spherical and smooth morphology, which is the same as that of the pristine one. Likewise, the morphologies of T-NCA and U-NCA are also the same (see Fig. S1 of the Supplementary materials). The EDS mapping results indicate the uniform distribution of Mn on the surface of the precursor and T-NCA.

The initial charge–discharge curves (0.1*C*) of U-NCA and T-NCA tested at room temperature and elevated-temperature are plotted in Fig. 3a and b, and the cycling performances (2*C*) of the two samples are shown in Fig. 3c and d. As can be seen in Fig. 3a and b, T-NCA exhibits an initial discharge capacity of 189 mAh g^{-1} at room temperature, which is almost the same as that delivered by U-NCA. Similarly, at 55 °C, T-NCA and U-NCA have nearly equal discharge capacities, which are about 203 mAh g^{-1}. Besides, the charge–discharge curves of U-NCA and T-NCA almost fully overlap, indicating that the electrochemical active couples (such as Ni^{2+}/Ni^{3+}, Ni^{3+}/Ni^{4+} and Co^{3+}/Co^{4+}) have not been varied when Mn dopes on the surface of $LiNi_{0.8}Co_{0.15}Al_{0.05}O_2$ cathode material. Fig. 3c displays the cycling performances of U-NCA and T-NCA at room temperature. Apparently, T-NCA shows better cyclic ability. After 200 cycles the U-NCA sample delivers 77.6 mAh g^{-1}, which is as much as 50.9% of its initial capacity. The T-NCA, by contrast, shows improved cycling performance, maintaining its discharge capacity of 99.5 mAh g^{-1} with the capacity retention of 62.9%. At 55 °C, as shown in Fig. 3d, the discharge capacity of U-NCA after 100 cycles is 84.4 mAh g^{-1} with a capacity retention of 49.3%. In Contrast, T-NCA delivers a capacity of 115.9 mAh g^{-1} after 100 cycles and its capacity retention is 67.5%. Therefore, the Mn-surface-modification can enhance the cycling stability both at room and elevated temperature.

Fig. 4a and b shows the EIS results of U-NCA and T-NCA respectively; each Nyquist plot presents two semicircles. The one in high frequency region reflects the surface film resistance (R_{sf}), and the other in medium-to-low frequency region is attributed to the charge-transfer resistance (R_{ct}). As seen in Fig. 4a, the R_{sf} of U-NCA tends to increase gradually as the cycle number increases (see the inset). And the radius of the medium-to-low frequency semicircle, relating to R_{ct}, increases from several tens ohms to about 650 Ω during the cycling. In Fig. 4b, however, the R_{sf} of T-NCA exhibits nearly consistent value (see the inset). Additionally, the R_{ct} value of T-NCA increases much slower than that of U-NCA. As can be seen, the radius of the medium-to-low frequency semicircle increases from several tens ohms to about 215 Ω. According to other reports [14,15], a constant value of R_{sf} is a reflection of a stable solid electrolyte interface (SEI) film, and the continued growth of R_{ct} is closely related to an increasing handicap for lithium ion and electron transport. The increment of impedance may result from the formation of unwanted resistive layers between the electrode and electrolyte, the pulverization of the electrode and the

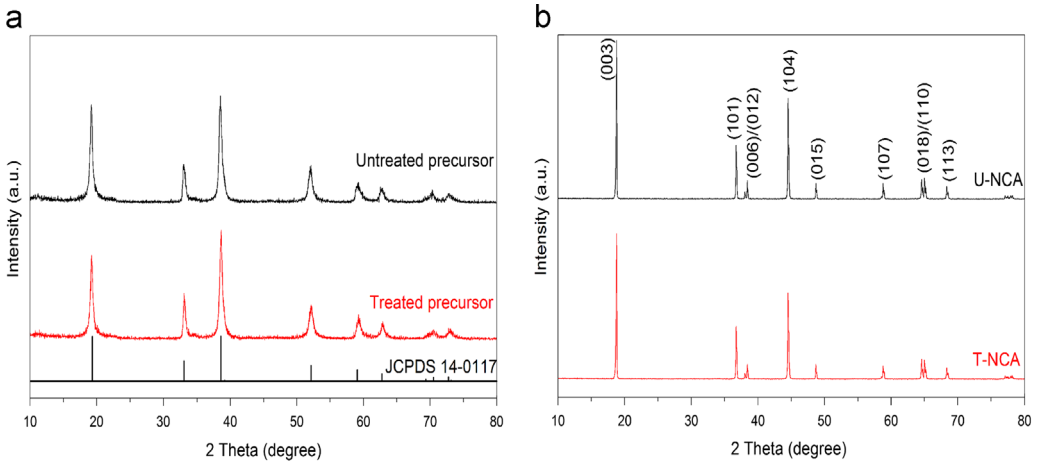

Fig. 1. XRD patterns of (a) untreated and $KMnO_4$ treated precursor, together with (b) the corresponding U-NCA and T-NCA.